

Synthesis and Characterization of Colorless Polyimide Nanocomposite Films Containing Pendant Trifluoromethyl Groups

Hyo-Seong Jin and Jin-Hae Chang*

Department of Polymer Science and Engineering, Kumoh National Institute of Technology, Gumi 730-701, Korea

Jeong-Cheol Kim

Gwangju R&D Center, Korea Institute of Industrial Technology, Gwangju 500-460, Korea

Received September 10, 2007; Revised March 10, 2008; Accepted March 10, 2008

Abstract: A series of colorless polyimide (PI) nanocomposite films were synthesized from 2,2'-bis(3,4-dicarboxyphenyl)hexafluoropropane dianhydride (6FDA) and 2,2'-bis(trifluoromethyl)-4,4'-diaminobiphenyl (TFDB) with various organoclay contents by solution intercalation polymerization to poly(amic acid)s, followed by thermal imidization. The variation with the organoclay content of the thermomechanical properties, morphology, and optical transparency of the hybrids was examined at organoclay loadings ranging from 0 to 1.0 wt%. The hybrid films showed high optical transparency and almost no color, with cut-off wavelengths ranging from 352 and 356 nm and very low b^* values of 1.19-1.77. The hybrid PI films showed good thermal properties with a glass transition temperature of 280-287 °C. Most films did not show any significant thermal decomposition below 490 °C. The addition of only a small amount of organoclay was sufficient to improve the tensile properties of the PI films with maximum enhancement being observed at 0.25 wt% organoclay. Moreover, these PI hybrids also had low coefficients of thermal expansion (CTE).

Keywords: colorless polyimide, film, nanocomposite, organoclay.

Introduction

Polyimides (PIs) are considered to be among the most important super-engineering materials because of their superior mechanical properties at elevated temperature due to their thermal stability. Recently, much research effort has been devoted to developing high performance PI materials with excellent thermomechanical properties, good solubility, and high optical transparency.¹⁻⁴ In particular, transparent PIs have been prepared using dianhydride and diamine monomers substituted with fluorine moieties in the side groups.⁵⁻⁹ Moreover, these colorless PIs were shown to have superior solubility, thermal stability, and optical transparency characteristics compared with other commercialized PIs. In addition, optically transparent PI films have many potential uses in electrooptical devices, flexible display substrates, and semiconductor applications.¹⁰⁻¹²

Nanoscale composites of polymers with organoclays have been studied extensively.¹³⁻¹⁵ Nanostructured materials often possess a combination of physical and mechanical properties not present in conventional polymer matrix composites.

Even at low clay contents (< 10 wt%), the thermomechanical properties of the polymer matrix can be substantially improved.¹⁶⁻¹⁸ Several methods have been used to obtain nanocomposites of polymers with organoclays, specifically solution intercalation, melt intercalation, and *in situ* interlayer intercalation. Among them, solution intercalation is based on a solvent system in which the polymer is soluble and the clay layers swell. The layered clay is first swollen in a solvent, such as *N,N*-dimethylacetamide (DMAc). When the polymer and clay solutions are mixed, the polymer chains intercalate and displace the solvent from between the layers of the clay. Upon solvent removal, the intercalated structure remains, resulting in hybrids with nanoscale morphology.^{19,20}

In accord with earlier observations by Pinnavaia,²¹ increasing *n*-alkyl chain length of alkylammonium compounds and ion-exchange with protonated primary amines resulted in much larger interlayer distances in these nanocomposites than in nanocomposites containing pristine clays. It appears likely that primary amines react with polyimides to facilitate development of products with alkyl chains, thus enhancing both swelling and compatibility.^{22,23}

Previous work in our laboratory has demonstrated the possibility of a nanocomposite of PI with organoclay and a high

*Corresponding Author. E-mail: changjinhae@hanmail.net

performance material in a precursor.^{24–26} Nanostructured materials often possess a combination of physical and mechanical properties not present in conventional composites. Even at low concentrations of clay content (< 10 wt%), the thermo-mechanical properties can be substantially increased, whereas gas permeability rate is reduced.

In the present study, we prepared a colorless PI hybrid by thermal imidization of an aromatic precursor polymer based on the reaction of 4,4'-(hexafluoroisopropylidene) diphthalic anhydride (6FDA) and 2,2'-bis(trifluoromethyl)-4,4'-diaminobiphenyl (TFDB). The objective of this study was to evaluate the effect of the organoclay in PI nanocomposites, as a hybrid system, as a function of the amount of organoclay. In this paper, we describe a method for making the colorless PI hybrids by using the solution intercalation method. Also, the thermomechanical properties, morphologies, and optical transparencies of the PI hybrid films are reported for various organoclay contents.

Experimental

Materials. Cloisite 25A (organically modified MMT) was obtained from Southern Clay Product, Co. All reagents were purchased from TCI (Tokyo, Japan) and Aldrich Chemical Co. (Yongin, Korea). 6FDA and TFDB were obtained from TCI, and were used as received. DMAc was purified and dried over molecular sieves before use. All other reagents were used without further purification.

Preparation of the Colorless PI Hybrid Films. Poly(amic acid) (PAA) was synthesized from 6FDA and TFDB in DMAc by the low temperature method.²⁷ TFDB (6.5 g; 2.0×10^{-2} mol) and DMAc (40 mL) were placed in a 100 mL three-necked flask, and the mixture was stirred at 0 °C for 30 min under a nitrogen atmosphere. 6FDA (9.0 g; 2.0×10^{-2} mol) in DMAc (50 mL) was then added. The resulting solution was stirred vigorously at 0 °C for 2 h, and then at room temperature for 13 h, yielding a 15 wt% DMAc solution of PAA.

Because the synthetic procedures used to produce the polymer/organoclay nanocomposites were the same for all Cloisite 25A contents, we only describe the preparation of PI/Cloisite 25A (0.50 wt%) as a representative example. A dispersion of 0.074 g Cloisite 25A, 14.9 g of PAA solution, and excess DMAc (30 mL) was stirred vigorously at room temperature for 24 h. The solution was cast onto glass plates, and then the solvent was evaporated in a vacuum oven at 50 °C for 2 h. The solvent-casted film was cleaned for many times in an ultrasonic cleaner three times for 5 min each time. These films with solvent removed were dried again in a vacuum oven at 60 °C for one day. The film thickness was about 100 μm . The PAA film was further imidized on the glass plate by sequential heating at 100, 150, and 200 °C for 1 h at each temperature, followed by 2 h at 250 °C.

All PIs exhibit the characteristic imide group absorptions around 1776 and 1724 cm^{-1} , asymmetric and symmetric stretch-

Table I. Thermal Properties of Polyimide Hybrid Films

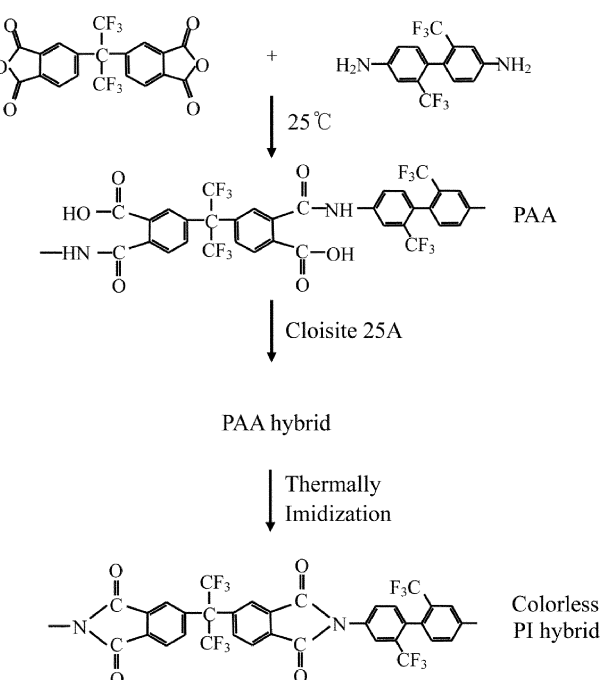
Cloisite 25A (wt%)	I.V. ^a	T _g (°C)	T _d ^b (°C)	wt _R ^{800c} (%)	CTE ^d (ppm/°C)
0 (pure PI)	0.59	278	489	50	55
0.25	0.61	283	516	50	50
0.50	0.65	287	523	50	48
0.75	0.60	284	504	50	51
1.00	0.57	280	492	50	52

^aInherent viscosities were measured at 30 °C by using 0.1 g/100 mL solution in a *N,N*-dimethylacetamide.

^bAt a 2% initial weight-loss temperature.

^cWeight percent of residue at 800 °C.

^dTemperature range for CTE is 100–250 °C.



Scheme I. Synthetic routes of colorless PI hybrids.

ing), 1365 cm^{-1} (C-N-C stretching) and 1114 cm^{-1} (imide ring). The lack of absorption in the region 2500–3500 cm^{-1} (O-H and N-H stretch) and around 1680 cm^{-1} (amide C = O stretch) indicates that the polymers were fully imidized.

The PIs are soluble in DMAc, which was the solvent used in the measurement of solution viscosity. The inherent viscosities of the resulting PI hybrid films in DMAc (see Table I) were found to range from 0.57 to 0.65, measured at a concentration of 0.1 g/dL at 30 °C. Considering that these viscosity values were obtained from pure PI in PI hybrids in which the clay contents had been removed, these numbers can be regarded as being constant. The chemical structures relevant to the synthetic route are shown in Scheme I.

No fixed tools were used for orientation on the glass plate during heat treatment because orientation can influence some

characteristics of film specimens, such as tensile properties and morphology.

Characterization. Wide-angle X-ray diffraction (XRD) measurements were performed at room temperature on a Rigaku (D/Max-IIIB) X-ray diffractometer, using Ni-filtered Cu-K α radiation. The scanning rate was 2°/min over a range of 2θ=2–12°. A differential scanning calorimeter (DSC 200F3) was used on a NETZSCH instrument and a thermogravimetric analyzer (AutoTGA 1000) was used on a TA instrument with a heating rate of 20 °C/min under N₂ flow. Measurement of the coefficient of thermal expansion (CTE) of the samples was performed with a macroexpansion probe (TMA-2940), which applied 0.1 N expansion force on the film, at a heating rate of 5 °C/min in the temperature range of 50–250 °C.

The tensile properties of the solution cast films were determined using an Instron Mechanical Tester (Model 5564) at a crosshead speed of 5 mm/min. The specimens were prepared by cutting strips with dimensions of 5 × 70 mm². Averages of at least ten individual determinations were used. The experimental uncertainties in tensile strength and modulus were ± 1 MPa and ± 0.05 GPa, respectively.

The morphologies of the fractured surfaces of the film samples were investigated using a Hitachi S-2400 scanning electron microscope. The fractured surfaces were sputter-coated with gold using an SPI Sputter Coater for enhanced conductivity. Transmission electron microscopy (TEM) photographs of ultrathin sections of the PI/Cloisite 25A hybrid films were obtained with a Leo 912 OMEGA transmission electron microscope using an acceleration voltage of 120 kV.

The color intensity of the polymer films was evaluated with a Minolta spectrophotometer (Model CM-3500d). The measurements were obtained for 100 μm thick films. Ultra-violet-visible (UV-vis) spectra of the polymer films were recorded on a SHIMDAZU UV-3600.

Results and Discussion

Organoclay Dispersion. Figure 1 shows the XRD patterns of the organoclay and pure PI, along with those of PI hybrid films with organoclay loadings ranging from 0.25 to 1.00 wt%. The XRD peak for the surface-modified clay, Cloisite 25A, was observed at 2θ=4.54°, which corresponds to an interlayer distance of 19.44 Å.

The PI hybrid with 0.25 wt% organoclay shows only a weak peak at $d = 12.76 \text{ \AA}$ ($2\theta = 6.92^\circ$). A substantial increase in the intensity of this XRD peak was observed for clay loadings in the range 0.25–1.00 wt%, suggesting that the peak intensity is smaller at lower clay loadings than at higher clay loadings and that agglomeration occurs at higher clay loadings. However, the presence of the organoclay was found to have no effect on the location of the peak, which indicates that perfect exfoliation of the clay layer structure of the organoclay in PI did not occur in these nanocomposites.²⁸ This also

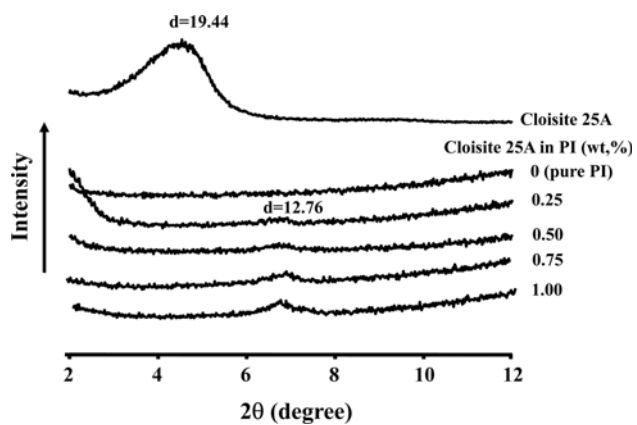


Figure 1. XRD patterns of Cloisite 25A and PI hybrids with various Cloisite 25A contents.

implies that a large amount of organoclay cannot be exfoliated in PI; it exists in the form of an intercalated layer structure.

Yano *et al.*²⁹ reported that organic molecules in the clay interlayers that interact only weakly with the clay might detach from the clay surface. This detachment by heat treatment occurs during the cyclization process from PAA to PI, and causes a reduction in the interlayer spacing from the basal spacing of organoclay (19.44 to 12.76 Å). This squeezing mechanism should also serve to inhibit exfoliation of the organoclay in the PI, causing the organoclay to exist in the form of an intercalated layer structure.

Morphology. Further evidence of organoclay dispersed in PI on the nanometer scale was provided by a morphological study. SEM images of the fractured surfaces of the PI hybrid films containing 0–1.00 wt% organoclay are compared in Figure 2. Figures 2(b) and (c) show that clay phases form in the PI hybrid films: the films with 0.25–0.50 wt% Cloisite 25A have morphologies consisting of clay domains that are well dispersed in a continuous PI phase. The particles of the dispersed clay phase were easily detected for clay contents up to 0.50 wt%. By contrast, the micrographs of the 0.75 and 1.00 wt% Cloisite 25A/PI hybrid film (Figures 2(d) and (e)) show voids and some deformed regions that can be attributed to the coarseness of the fractured surface. Comparison of the micrographs shows that the fractured surfaces of the hybrid films with higher clay contents are more deformed than those of the films with lower clay contents, possibly due to the agglomeration of clay particles. This hypothesis is supported by the observation of agglomerated clay particles in the PI hybrid films with clay contents of 0.75 and 1.00 wt%.

To more precisely examine the dispersion of the clay layers in the film hybrids, we carried out TEM studies. TEM affords a qualitative understanding of the internal structure through direct observation. Typical TEM photographs of hybrid with 0.5 wt% Cloisite 25A contents are shown in Figure 3. The dark lines are the intersections of 1 nm-thick sheet layers. The TEM photographs show that the clay is dispersed

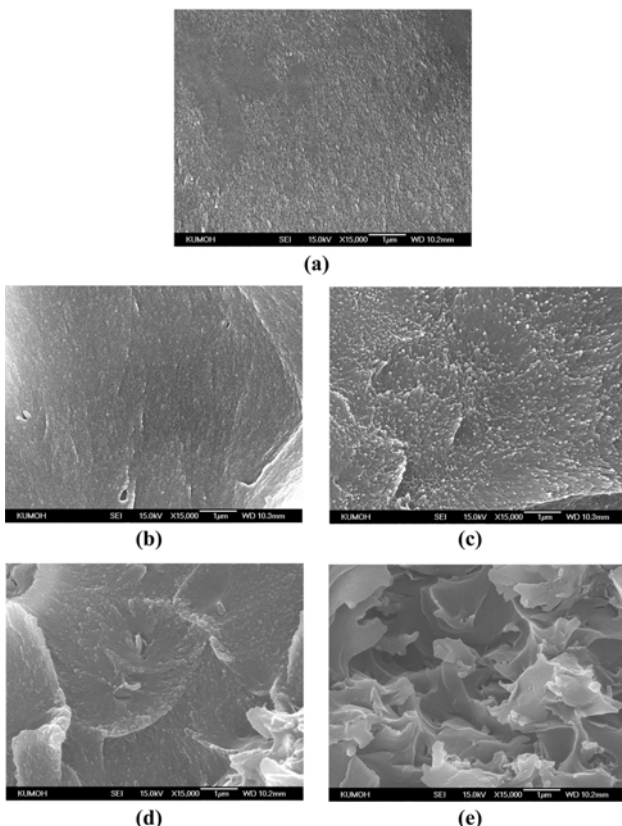


Figure 2. SEM photographs of PI/Cloisite 25A hybrids containing (a) 0 (pure PI), (b) 0.25, (c) 0.50, (d) 0.75, and (e) 1.00 wt % of Cloisite 25A.

in the polymer matrix at all magnification levels, although some clusters or agglomerated particles are also detected, indicating that nanocomposites have formed. The presence of peaks in the XRD patterns of these samples should be attributed to these agglomerated layers (see Figure 1).

On the basis of the preceding results, we can conclude that the state of the clay particles affected the thermal behavior and the tensile mechanical properties of each polymer/clay hybrid. In films with low clay contents (0.50 wt%), the clay particles may be better dispersed in the polymer matrix without a large degree of particle agglomeration, compared to particles in films with high clay contents.³⁰ However, agglomerated structures form and become denser in the PI matrix above 0.75 wt% clay content. This is also consistent with the XRD and SEM results shown in Figures 1 and 2.

Thermal Behavior. Table I presents the thermal behavior of pure PI and its hybrid films obtained by solution polymerization with various clay contents. The glass transition temperatures (T_g) of the pure PI hybrids increase from 278 to 287 °C with increase in the clay loading from 0 to 0.50 wt%. This increase in T_g is ascribed to the confinement of the intercalated polymer chains within the clay galleries, which prevents segmental motions of the polymer chains.³¹⁻³³ However,

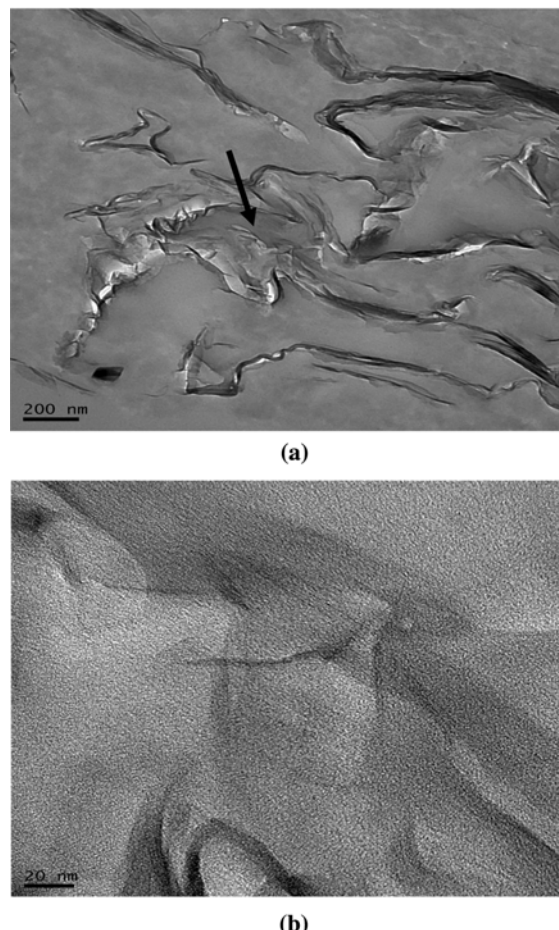


Figure 3. TEM micrographs of 0.5 wt% Cloisite 25A in PI hybrid films increasing the magnification levels from (a) to (b).

the maximum transition peaks of the PI hybrids increase with the addition of clay up to a critical content, and then decrease above that critical loading. For example, the T_g of the 0.75 wt% PI hybrid is 284 °C. When the organoclay content in PI reaches 1.00 wt%, the T_g is 280 °C. This decrease in T_g seems to be the result of clay agglomeration, which occurs on the addition of clay into the polymer matrix above a critical clay loading. DSC thermograms of the pure PI and the hybrids are shown in Figure 4. The presence of clay agglomeration in PI was already confirmed using XRD and SEM (see Figures 1 and 2).

The initial thermal degradation temperatures (T_D^i) of the PI hybrid films were also found to increase linearly from 489 to 523 °C as the organoclay loading was increased from 0 to 0.50 wt% (see Table I). The presence of the clay also enhances the initial decomposition temperatures by acting as an insulator and as a mass-transport barrier to the volatile products generated during decomposition.^{34,35} This increase in the thermal stability can also be attributed to the high thermal stability of the clay and to the interactions between the clay particles and the polymer matrix. However, the T_D^i value of

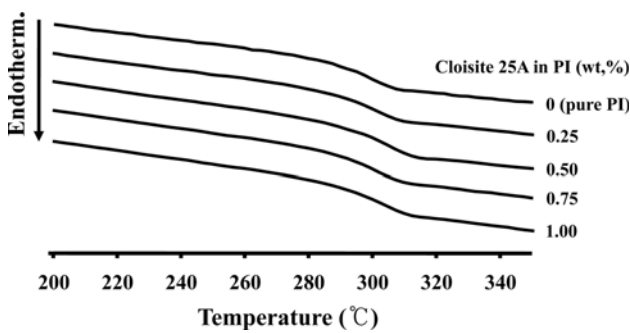


Figure 4. DSC thermograms of PI hybrids with various Cloisite 25A contents.

the PI hybrid films with 1.00 wt% clay loading (492°C) is lower by 31°C compared with those of the PI hybrid containing 0.50 wt% organoclay (523°C). This decrease in T_D^i seems to be the result of clay agglomeration. The results of weight residue measurements at 900°C (wt_R^{900}) show almost the same values regardless of the clay loading, as shown in Table I.

The values of the CTE in the temperature range $100\text{--}250^{\circ}\text{C}$ of the PI hybrids are listed in Table I. The CTEs of the PI hybrids decreased with the addition of clay up to a critical content, and then increased above that critical loading. For example, the CTEs of the PI hybrids decreased from 55 to 48 ppm/ $^{\circ}\text{C}$ with increase in the clay loading from 0 to 0.50 wt%. This observation means that the amount of the reduction of thermal expansion by the clay layers depends on the orientation of the PI molecules and the rigid nature of the clay layers. Upon heating, the in-plane oriented PI molecules tend to relax in a direction normal to their original direction and therefore expand mainly in the out-of-plane direction. The clay layers are much more rigid than the PI molecules, and they do not deform or relax as easily as the PI molecules do. Consequently, the clay layers very effectively retarded the thermal expansion of the PI molecules in the out-of-plane direction.³⁶⁻³⁸ However, the values of the CTEs increased above this content (> 0.5 wt%). This increase in CTE seems to be the result of clay agglomeration. These results are also supported by the T_g and T_D^i data mentioned above (Table I).

Mechanical Properties. The tensile mechanical properties of the PI and hybrid films are listed in Table II. The ultimate tensile strength and the initial tensile modulus of the PI hybrid films were found to increase from 105 to 135 MPa and from 2.99 to 3.43 GPa, respectively, as the clay loading was increased from 0 to 0.25 wt% (see Table II). This enhancement of the tensile properties is ascribed to the high resistance exerted by the clay. Further, the increased stretching resistance of the polymer chains produced by the orientation of their backbones in the galleries also contributes to the enhancement of the mechanical properties.

In contrast to the behavior observed for Cloisite 25A contents of 0 to 0.25 wt%, the mechanical values of the hybrids

Table II. Tensile Properties of Polyimide Hybrid Films

Cloisite 25A (wt%)	Ult. Str. (MPa)	Ini. Mod. (GPa)	E.B. ^a (%)
0 (pure PI)	105	2.99	6
0.25	135	3.43	6
0.50	118	3.13	5
0.75	108	3.08	5
1.00	106	3.01	6

^aElongation percent at break.

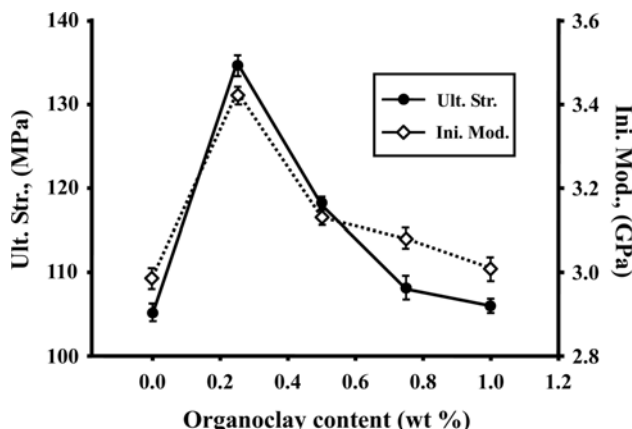


Figure 5. Effect of the clay loading on the ultimate strength and initial modulus of the PI hybrid films.

decrease with increasing the organoclay content from 0.50 to 1.00 wt%. For example, the ultimate strength and initial modulus values of the PI hybrid films with 1.00 wt% clay loading are lower by 29 MPa and 0.42 GPa, respectively, compared with those of the PI hybrid containing 0.25 wt% organoclay. This decrease in ultimate strength and initial modulus seems to be the result of clay agglomeration, which occurs when the clay content in the polymer matrix exceeds some critical value. The variations of the ultimate strengths and initial moduli of the PI hybrids are plotted against organoclay content in Figure 5.

In contrast to the mechanical properties, the percent elongations required to break the hybrid films remained fairly constant in the range of 5-6% with variation of the clay loading from 0-1.00 wt%, as shown in Table II.

Optical Transparency. The color intensities of the PI hybrid films with various Cloisite 25A contents are listed in Table III. For comparison, Kapton® 200KN film, which is based on pyromellitic dianhydride (PMDA) and oxydianiline (ODA), was also characterized by its color intensity. Table III shows that the color intensity of the PI hybrid films was affected by the organoclay content. Table III also shows that PI hybrid films with lower organoclay content had lower b^* values than those of the corresponding hybrids with higher organoclay content. The b^* value of the PI hybrid with

Table III. Color Coordinates of Polyimide Hybrid Films

Cloisite 25A (wt%)	Film Thickness (μm)	L* ^a (White-Black)	a* ^b (Red-Green)	b* ^c (Yellow-Blue)	λ _θ ^d (nm)
0 (pure PI)	100	96.24	-0.41	1.17	350
0.25	100	96.23	-0.36	1.19	352
0.50	100	96.08	-0.43	1.45	353
0.75	100	95.90	-0.47	1.63	355
1.00	100	96.08	-0.50	1.77	356
Kapton® 200KN	52	79.44	21.12	106.27	442

^aAn L of 100 is white, and 0 is black. ^bA positive a* of indicates red, and a negative a* indicates green. ^cA positive b* of indicates yellow, and a negative b* indicates blue. ^dCut-off wavelength.

Poly(amic acid) was synthesized by means of low-temperature of 3,3'-dihydroxybenzidine and pyromellitic dianhydride. The precursor polymer was heat-treated at different temperaturebenzoxazole (PBO) through a polyimide (PI). PI contain rearranged by decarboxylation with heat treatment, resulting in PBO. Hexadecylamine was used as an organophilic alkylamine to clarify the intercalation of heterocyclic polymer chains montmorillonite (C_{16} -MMT) and improve tensile properties. It was only a small amount of organo-clay was enough to improve of PBO. Maximum enhancement in the ultimate tensile strength was observed for the blends containing 4% C_{16} -MMT. The intensity increased with further increases in the C_{16} -MMT content.³⁸ Inc. J Polym Sci B: Polym Phys 39: 471–476, 2001

Poly(amic acid) was synthesized by means of low-temperature of 3,3'-dihydroxybenzidine and pyromellitic dianhydride. The precursor polymer was heat-treated at different temperaturebenzoxazole (PBO) through a polyimide (PI). PI contain rearranged by decarboxylation with heat treatment, resulting in PBO. Hexadecylamine was used as an organophilic alkylamine to clarify the intercalation of heterocyclic polymer chains montmorillonite (C_{16} -MMT) and improve tensile properties. It was only a small amount of organo-clay was enough to improve of PBO. Maximum enhancement in the ultimate tensile strength was observed for the blends containing 4% C_{16} -MMT. The intensity increased with further increases in the C_{16} -MMT content.³⁸ Inc. J Polym Sci B: Polym Phys 39: 471–476, 2001

Poly(amic acid) was synthesized by means of low-temperature of 3,3'-dihydroxybenzidine and pyromellitic dianhydride. The precursor polymer was heat-treated at different temperaturebenzoxazole (PBO) through a polyimide (PI). PI contain rearranged by decarboxylation with heat treatment, resulting in PBO. Hexadecylamine was used as an organophilic alkylamine to clarify the intercalation of heterocyclic polymer chains montmorillonite (C_{16} -MMT) and improve tensile properties. It was only a small amount of organo-clay was enough to improve of PBO. Maximum enhancement in the ultimate tensile strength was observed for the blends containing 4% C_{16} -MMT. The intensity increased with further increases in the C_{16} -MMT content.³⁸ Inc. J Polym Sci B: Polym Phys 39: 471–476, 2001

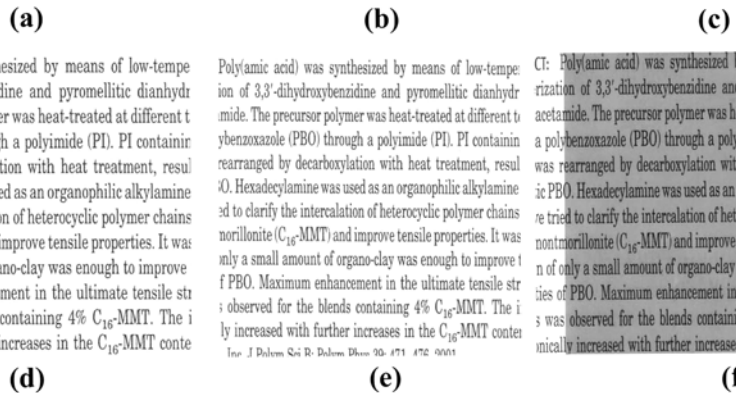


Figure 6. Photographs of PI hybrid films containing (a) 0 (pure PI), (b) 0.25, (c) 0.50, (d) 0.75, and (e) 1.0 wt % of Cloisite 25A. Kapton® 200KN was shown in (f) as a reference.

0.25 wt% organoclays was 1.19, and its degree of colorlessness is almost the same as that of aliphatic poly(methyl methacrylate) (PMMA) ($b^* = 1.2$).⁶ When the clay loading was increased to 0.50 and then to 1.00 wt%, no significant increases in the b^* value were observed. The color intensities of the hybrid films could also be elucidated from the cutoff wavelength (λ_θ) observed in the UV-vis absorption spectra. The fluorinated PI (6FDA/TFDB) and its hybrid film showed a shorter λ_θ than nonfluorinated Kapton (PMDA/ODA) (see Table III). The λ_θ values of the PI hybrids were virtually unchanged with variation in organoclay loading; specifically, they increased from 350 to 356 nm as the Cloisite 25A content increased from 0 to 1.00 wt%. These colorless PI films showed a UV transmittance by the

upper level of almost 90% at 450 nm and excellent optical properties. Compared with the colorless PI hybrid films, Kapton® 200 KN shows poor optical transparency, as shown in Table III.

The solvent cast hybrid films with organoclays contents in the range of 0–1.0 wt% were all almost colorless and transparent, as shown in Figures 6(a–e), indicating that the addition of the organoclays to the PI matrix did not significantly affect the transparency. These findings suggest that, even at an organoclay loading of 1.0 wt%, the phase domains in the hybrid film are significantly smaller than the wavelength of visible light.^{24,39} Thus, the hybrid films prepared in the present work exhibit excellent transparency due to a good dispersion of clay particles in the polymer matrix, although the transpar-

ency diminishes slightly with increasing organoclay content due to agglomeration of the clay particles.

Conclusions

PI/Cloisite 25A hybrid films were synthesized from 6FDA and TFDB with various organoclay contents using the solution intercalation method. The PI hybrid films containing a pendant CF₃ group showed shorter λ_0 and higher optical transparency than films of nonfluorinated PIs such as Kapton films. Electron-withdrawing CF₃ groups in the diamine as well as the dianhydride moieties were presumably effective in decreasing the charge transfer complex between polymer chains through steric hindrance and the inductive effect. Moreover, these PI hybrid films were fairly transparent and almost colorless. The cast hybrid films also exhibited good thermal stability and mechanical tensile properties, and are expected to be usable as high-performance polymeric materials.

Acknowledgements. This research was supported by Research Fund, Kumoh National Institute of Technology.

References

- (1) W. Qu, T. Z. Ko, R. H. Vora, and T. S. Chung, *Polymer*, **42**, 6393 (2001).
- (2) C. P. Yang and H. W. Yang, US Patent 6,093,790 (2000).
- (3) A. K. S. Clair and W. S. Slemp, *SAMPE J.*, **21**, 28 (1985).
- (4) B. Y. Myung, J. S. Kim, and T. H. Yoon, *J. Polym. Sci. Part A: Polym. Chem.*, **41**, 3361 (2003).
- (5) C. P. Yang, R. S. Chen, and K. H. Chen, *Part A: J. Polym. Sci. Polym. Chem.*, **41**, 922 (2003).
- (6) C.-P. Yang and Y. Y. Sue, *Polymer*, **46**, 5778 (2005).
- (7) S. L. Ma, Y. S. Kim, J. H. Lee, J. S. Kim, I. Kim, and J. C. Won, *Polymer(Korea)*, **29**, 204 (2005).
- (8) C.-P. Yang and Y.-C. Chen, *J. Appl. Polym. Sci.*, **96**, 2399 (2005).
- (9) J. H. Kim, W. J. Koros, and D. R. Paul, *Polymer*, **47**, 3094 (2006).
- (10) A. S. Mathews, I. Kim, and C.-S. Ha, *Macromol. Res.*, **15**, 114 (2007).
- (11) K. Higashi and Y. Noda, Eur Pat. 240249 (1986).
- (12) T. Matsuura, S. Ando, S. Sasaki, and F. Yamamoto, *Electron. Lett.*, **29**, 2107 (1993).
- (13) G. Lagaly, *Appl. Clay Sci.*, **15**, 1 (1999).
- (14) E. P. Giannelis, *Adv. Mater.*, **8**, 29 (1996).
- (15) K. H. Kim, K. H. Kim, J. Huh, and W. H. Jo, *Macromol. Res.*, **15**, 178 (2007).
- (16) M. A. Osman, V. Mittal, M. Morbidelli, and U. W. Suter, *Macromolecules*, **36**, 9851 (2003).
- (17) R. K. Bharadwaj, *Macromolecules*, **34**, 9189 (2001).
- (18) Z.-M. Liang and J. Yin, *J. Appl. Polym. Sci.*, **90**, 1857 (2003).
- (19) D. G. Greenland, *J. Colloid Sci.*, **115**, 40 (1970).
- (20) Z. Shen, G. P. Simon, and Y.-B. Cheng, *Polymer*, **43**, 4251 (2002).
- (21) T. J. Pinnavaia, *Science*, **220**, 365 (1983).
- (22) A. Okada and A. Usuki, *Mater. Sci. Eng.*, **C3**, 109 (1995).
- (23) Y. Yang, Z. Zhu, J. Yin, X. Wang, and Z. Qi, *Polymer*, **40**, 4407 (1999).
- (24) J.-H. Chang, D. K. Park, and K. J. Ihn, *J. Appl. Polym. Sci.*, **84**, 2294 (2002).
- (25) J.-H. Chang and K. M. Park, *Polym. Eng. Sci.*, **41**, 2226 (2001).
- (26) J.-H. Chang, K. M. Park, D. Cho, H. S. Yang, and K. J. Ihn, *Polym. Eng. Sci.*, **41**, 1514 (2001).
- (27) J.-H. Chang and K. M. Park, *Eur. Polym. J.*, **36**, 2185 (2000).
- (28) A. B. Morgan and J. W. Gilman, *J. Appl. Polym. Sci.*, **87**, 1329 (2003).
- (29) K. Yano, A. Usuki, A. Okada, T. Kurauchi, and O. Kamigaito, *J. Polym. Sci. Part A: Polym. Chem.*, **35**, 2289 (1997).
- (30) H. S. Jin and J.-H. Chang, *J. Appl. Polym. Sci.*, **107**, 109 (2008).
- (31) J.-H. Chang, B.-S. Seo, and D.-H. Hwang, *Polymer*, **43**, 2969 (2002).
- (32) F. Li, J. Ge, P. Honigfort, S. Fang, J. C. Chen, F. Harris, and S. Cheng, *Polymer*, **40**, 4987 (1999).
- (33) T. Agag and T. Takeichi, *Polymer*, **41**, 7083 (2000).
- (34) T. D. Fornes, P. J. Yoon, D. L. Hunter, H. Keskkula, and D. R. Paul, *Polymer*, **43**, 5915 (2002).
- (35) X. S. Petrovic, L. Javni, A. Waddong, and G. J. Banhegyi, *J. Appl. Polym. Sci.*, **76**, 133 (2000).
- (36) H.-L. Tyan, Y.-C. Liu, and K.-H. Wei, *Chem. Mater.*, **11**, 1942 (1999).
- (37) T. Agag, T. Koga, and T. Takeichi, *Polymer*, **42**, 3399 (2001).
- (38) M. Okamoto, S. Morita, Y. H. Kim, T. Kotaka, and H. Tateyama, *Polymer*, **42**, 1201 (2001).
- (39) K. Yano, A. Usuki, A. Okada, T. Kurauchi, and O. Kamigaito, *J. Polym. Sci. Part A: Polym. Chem. Ed.*, **31**, 2493 (1993).